WHEEL SLIP MEASUREMENT OF AN ELECTRIC VEHICLE PROTOTYPE USING AN ACCELEROMETER

Eng. **Daniel SZÖCS** PhD candidate[1], Eng. **Andrei FENEŞAN** PhD candidate[1],
Prof. Eng. **Teodor PANĂ** PhD[1]

[1]Technical University of Cluj-Napoca, Electrical Engineering Faculty,
Department of Electrical Machines and Drives

REZUMAT. Pentru şoferii de automobile cât şi pentru manufacturieri, siguranţa automobilului este de mare importanţă. Derapajul la roată este un factor în siguranţa şi performanţa vehiculului. Se cercetează determinarea diferenţelor de viteză între roti şi vehicul, folosind un accelerometru şi encodere. Se exemplifică metode de compensare şi calibrare a acceleraţiei gravitaţionale, necesare pentru determinarea vitezei vehiculului. Derapajul la roată se simulează şi observă experimental.

Cuvinte cheie: derapaj la roată, viteză, accelerometru, gravitație

ABSTRACT. Vehicle safety is a great concern for automotive drivers and manufacturers. Wheel slip is a factor in safety, also in performance. Determination of wheel speed differences to the vehicle speed through an accelerometer and encoders is reaserched. Methods of compensation and calibration of gravitational acceleration are exemplified, necessary for vehicle speed determination. Wheel slip is simulated and experimentally observed.

Keywords: wheel slip, speed, accelerometer, gravity

1. INTRODUCTION

Traction control technology is paramount to vehicle safety in slippery road conditions. Observing wheel slip is the first step in creating a system that controls in real time or prevents large differences between vehicle and wheel speed. An active slip control would not only benefit safety, but also reduce costs of maintenance by reducing rubber ware. A system that is able to control wheel speed is also applicable in braking, as an anti-locking system.

Wheel speed estimation is not an issue; an encoder can precisely read the position. Vehicle speed, however, is proving to be a challenge. A free wheel with an encoder reading the speed values would be a simple solution, except in the case when breaking is done at that wheel. Using an accelerometer would seem like an alternative, but as will be presented, it is not the simplest solution, nor is it the most precise in itself. It raises a number of issues including computational needs and reliability. Wheel slip is measured experimentally using an electric vehicle prototype.

Current technologies are optimized for use on conventional Ackerman steering[1], petrol based vehicles. Slipping is controlled by varying brake force, thus affecting the vehicle speed parameter. Other methods include active torque distribution, like the ones used in four-wheel drive transmission systems. The advantage of individual torque control is that adhesion to the surface is distributed accordingly to the individual wheel and road slip coefficient. This way, slip control can be achieved quicker, more precisely and in some cases without the need for mathematical computation. When cornering, torque can be electronically controlled so that the outer wheels don't lose traction and allows for high speed cornering.

Traction control methods

Traction control can be classified into the following: longitudinal control improves adhesion by controlling the traction force, and lateral control of yaw by varying the steering angle. Recently a lot of electric vehicles have been developed, mainly hybrid models using both electric and fossil fuel energy. The main catalyst for the development of electric vehicles is to solve current energy and environmental issues caused by combustion engine vehicles (ICV). Electric motors have instantaneous high torque, quickly and precisely controlled as opposed to internal combustion engines.

One paper[2] proposes two methods for traction control for electric vehicles: "Model Following Control (MFC)" and "Optimal Slip Ratio Control". In the MFC, the actual speed is compared to the simulated speed output of the vehicle model; motor torque is reduced and traction is increased.

The side force has a maximum value when λ=0 and decreases rapidly for bigger λ. Sudden decrease of road friction causes λ to increase, the side force decreases as well. This has serious consequences: front wheel drive cars drift, rear wheel drive cars spin, and four wheel drive cars drift and rotate.

In the Optimal Slip Ratio Control, the road condition estimator decides the optimal slip ratio, the slip ratio controller uses this information to control the torque and obtain the desired slip ratio.

Slip ratio is defined as:

$$\lambda = \frac{(V_W - V)}{V_W} \quad (1)$$

where V_W is wheel speed and V is vehicle speed.

The kinematic equations of the wheel and of the vehicle are as follow:

$$(F_m - F_d)/(M_W \cdot s) = V_W \quad (2)$$

$$F_d/(M \cdot s) = V \quad (3)$$

where F_m is motor torque (force equivalent); F_d is friction force; M_W is wheel inertia (mass equivalent); M is vehicle weight.

The vehicle body can be seen as one inertia system with equivalent inertia moment J, by introducing the scalar slip ratio λ,

$$J = J_W + M \cdot r^2 \cdot (1 - \lambda) \quad (4)$$

where J_W, M and r are the shaft inertia moment, vehicle weight and tire radius.

Wheel slip ratio control for electric vehicle

The principle of the wheel slip controller for the electric vehicle prototype Robotics Starter Kit is the following: when slip coefficient values exceed a certain value, the behavior of the active wheel is changed to increase grip. A PID controller imposes a rotational speed correction for the wheels and traction is regained (Fig. 1).

The desired wheel speed is the command for the rotational speed of the wheel. The encoder speed is the speed measured by the optical encoder on the motor[3]. Sensor speed is the speed from the integrated acceleration sensor values. The sensitivity of the motor controller that commands the motor by translating PWM signal width to rotor speed is neglected in this model. This means the desired wheel speed and the encoder speed are considered to have the negligible differences. This is not true for small values of desired wheel speed, where small PWM command values are unable to determine motor spin.

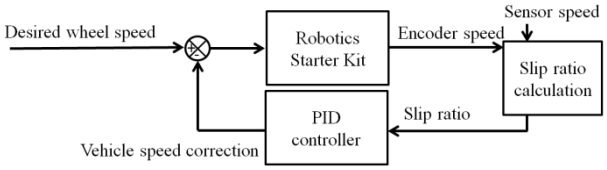

Fig. 1. Wheel slip ratio controller for the Robotics Starter Kit electric vehicle prototype.

2. ELECTRIC VEHICLE PROTOTYPE COMPONENTS AND FUNCTIONALITY

The electric vehicle prototype NI Robotics Starter Kit™ (Fig. 2) is comprised of a sbRIO9631 embedded device with AI, AO, DIO, 1M Gate FPGA. The programming is realized using the LabVIEW™ graphical development environment, programs are compiled using Xilinx™ tools and written to field programmable-gate arrays (FPGAs) on NI reconfigurable I/O hardware through the Ethernet port.

Digital I/O Port P2 is connected to a mezzanine board, which further connects to the motors controller, encoder sensors, ultrasonic sensors and its servomotor controller. A 12(V), 3000(mAh) Ni-MH battery serves as a power supply and a 12(V)-24(V) DC converter adjusts the power requirements for the sbRIO9631. Two motors are powered and controlled by a dual RC servo motor controller. The type of the motors is continuous-rotation servo. Rotation is sent to the wheel using a 2:1 gear ratio.

Motors are two RC servo controlled continuously rotating motors. A PWM signal is generated to control the motors: 1000(μs) pulse width corresponds to full backward speed, 1500(μs) to motor stop and 2000(μs) to full forward speed. Only the pulse width affects the speed, not the amplitude or the frequency. The duty cycle and current amperage affect torque. Amplitude of current dictates the amplitude of torque, and the duty cycle affects the jerkiness of the torque. For example, a 0.5 duty cycle means half of the time torque will be one hundred percent and half of the time it will be zero. Frequency of the signal affects the command rate, or how often one can change the command in a period of time.

The signal command is generated through ports DIO4 and DIO5 for the left and right motor respectively. Note that the motors have opposite motor movement, due to the opposite physical position of the motors shaft, this affects the PWM command.

Rotary optical encoders, one for each of the two motors, give absolute position feedback with 400 position increments. Data is sent through DIO0, DIO1 for the left motor and DIO2, DIO3 for the right.

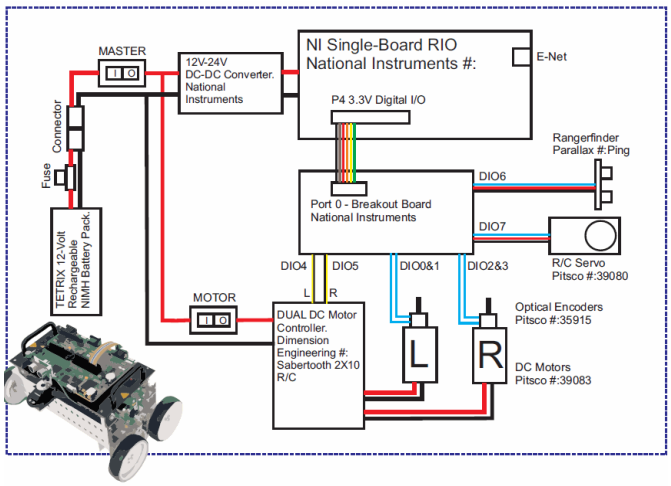

Fig. 2. LabVIEW Robotics Starter Kit block diagram.

In LabVIEW™, forward and angular velocity are transformed into left and right wheel velocities. A differential steer and fixed wheel frame is defined, wheel radius, wheel base and ratio are set.

SLIP SIMULATION IN MATLAB/SIMULINK

The vehicle is modeled using equations (1), (2), (3) and the Matlab/Simulink graphical programming environment. From the vehicle and wheel model as well as a given motor torque, we determined wheel drift.

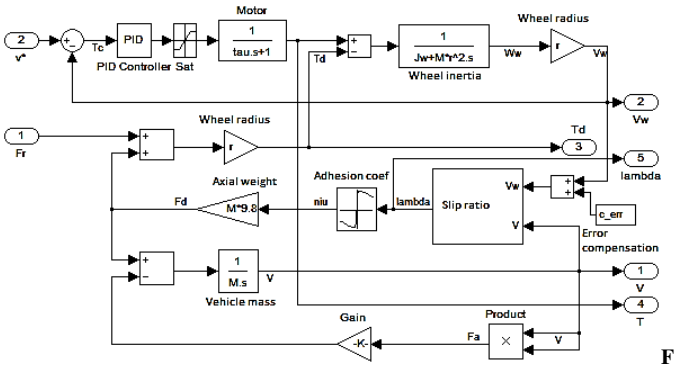

ig. 3. Vehicle model structure in Simulink. Generates wheel and vehicle speed and determines the slip ratio.

The following parameters have been defined:

Table 1

Simulation parameter name	Value(unit)
resistant wheel friction force, F_r	6.125(Nm)
wheel radius, r	0.0508(m)
wheel inertia moment, J_w	0.00077(kg·m^2),
vehicle mass, M	3.6(kg)
air density, ρ_a	1.205(kg/m^3)
air friction coefficient, c_{fa}	0.3
front vehicle area, A	0.035(m^2).

From 0 to 800(ms) there is an acceleration interval where the vehicle accelerates to the maximum speed: 0.3(m/s) (Fig. 4) and the torque is at maximum constant value (Fig. 5).

Speed is constant from 800 to 1000(ms); motor torque decreases and has same value as resistant torque. Until the 1550(ms) mark, the vehicle brakes and stops, motor torque is negative and less than resistant torque. Total simulation time is two seconds.

In figure 7, the μ–λ characteristic used in the simulation is generated by interpolating discrete values in a reference table. Wheel speed, vehicle speed, motor torque and resistant torque are the main parameters defining the vehicle behavior. Using (1), slip coefficient is found (Fig. 6).

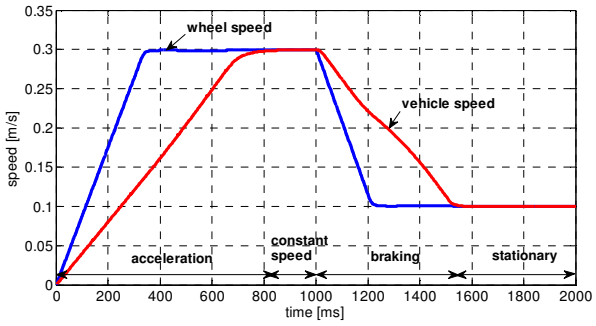

Fig. 4. Wheel and vehicle speed characteristic simulation in Simulink; four phases of movement: acceleration, constant speed, braking and stationary.

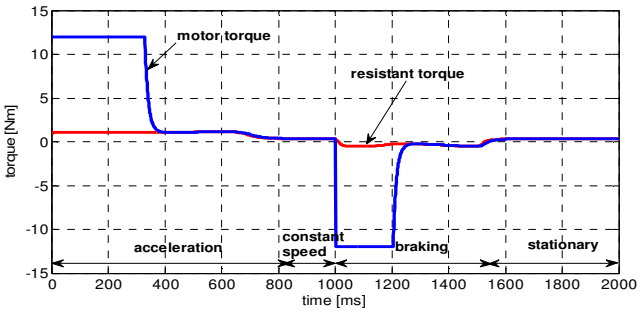

Fig. 5. Motor and resistant torque characteristic simulation in Simulink.

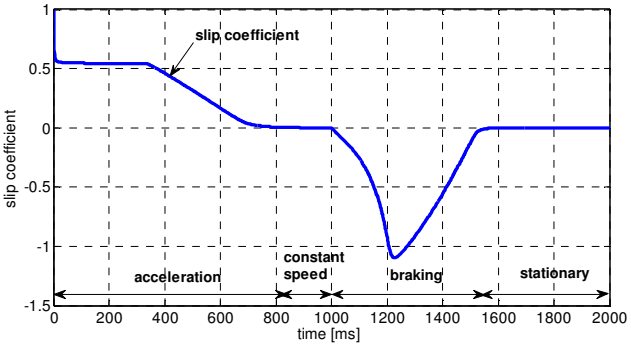

Fig. 6. Slip coefficient characteristics simulation in Simulink.

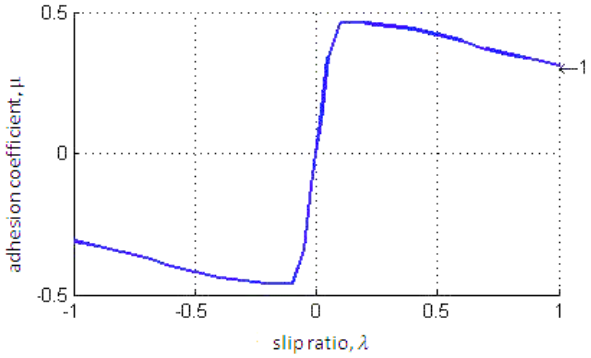

Fig. 7. Adhesion coefficient as a function of slip ratio, by interpolating discrete values in a reference table.

SPEED FROM ACCELEROMETER DATA INTEGRATION

Sensors are provided from an LG P970 smartphone and data is transmitted via Bluetooth.

Using an Android application called SendSensor, acceleration and orientation data is transmited via Bluetooth.

Raw acceleration data contains the gravitational acceleration as well as inertial linear acceleration. From the acceleration data, the gravitational component is removed by means of orientation compensation and the result is linear acceleration.

Gravity Compensation (Inertial Acceleration)

The Euler angles are a set of three angles that describe a number of three consecutive rotations around predefined axes. The mobile device that contains an accelerometer, also gives Euler angle values for an *XYZ* type rotation. It has a particular condition, which is that the final orientation is generated using only the first two rotations, meaning the rotation around z is considered null.

Rotation matrices describe rotation around a particular axis. By multiplying them, we get a generalized rotation matrix that is comprised of a rotation around x by φ degrees, then around y by θ degrees and lastly around z by ψ degrees.

$$R_x(\psi)R_y(\theta)R_z(\varphi) = \begin{bmatrix} R_{00} & R_{01} & R_{02} \\ R_{10} & R_{11} & R_{12} \\ R_{20} & R_{21} & R_{22} \end{bmatrix} \quad (5)$$

where, for an *XYZ* type rotation and considering the rotation around z to be null, we obtain:

$$\begin{cases} R_{00} = \cos\theta\cos\varphi \\ R_{01} = -\cos\theta\sin\varphi \\ R_{02} = \sin\theta \\ R_{10} = \sin\varphi \\ R_{11} = \cos\varphi \\ R_{12} = 0 \\ R_{20} = -\cos\varphi\sin\theta \\ R_{21} = \sin\theta\sin\varphi \\ R_{22} = \cos\theta \end{cases} \quad (6)$$

By multiplying the rotation matrix with the gravitational vector, we get the projections of the gravitational acceleration on the three axes.

$$\begin{bmatrix} R_{00} & R_{01} & R_{02} \\ R_{10} & R_{11} & R_{12} \\ R_{20} & R_{21} & R_{22} \end{bmatrix} \times \begin{bmatrix} 0 \\ 0 \\ g \end{bmatrix} = \begin{bmatrix} g_x \\ g_y \\ g_z \end{bmatrix} \quad (7)$$

Now that the gravitational acceleration has been determined, we apply the difference between the accelerometer readings and gravitational acceleration to obtain pure inertial acceleration. This is also called gravity compensation.

Prior to compensation, the accelerometer is calibrated for latitude and altitude influences[4], also the amplitude is calibrated using the two point formula[5]:

$$a_{xcal} = ma_x - n \quad (8)$$

where m is the slope and n is the intercept.

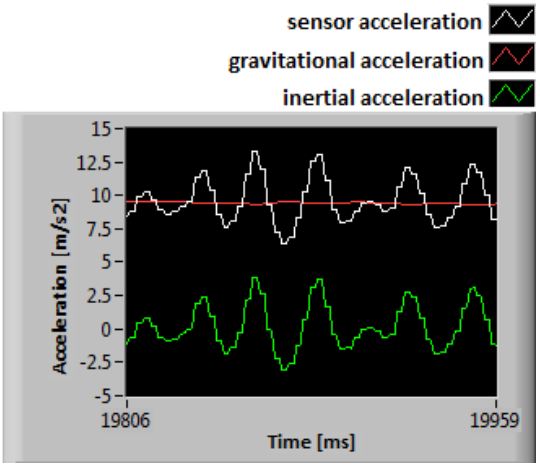

Fig. 8. Sensor acceleration in the x direction, contains raw sensor data (combined acceleration); gravitational component and inertial component.

In figure 8, the mobile device was oriented with the x axis oriented perpendicular to the ground and pointing downward. The variations in acceleration are caused by moving the phone up and down along its x axis. *Sensor acceleration* is the raw data from the sensor; *gravitational acceleration* has a constant value as long

as the sensor moves parallel to the ground plane; *inertial acceleration* or linear acceleration along one axis is the acceleration generated by movement.

Speed by Integration

By integrating the linear acceleration along the x axis, linear speed results:

$$\int [a_x(t) + err_{n.x}(t)]\, dt = v_x(t) + coeff_{drift.x}(t) + C \quad (9)$$

A simplified version is point by point integration, dividing two small variations in one period of time. Last acceleration value is given at the beginning of the new period and measured again in the current. Subtracting the last value from the previous gives us a measure of acceleration in one period of time. Times values are also subtracted, present time from last period time. Shift registers are used for this purpose.

Initial conditions are $v_{x0}=0$ and $t_0=0$.

$$a_{x1}=v_{x1}/t_1 \quad (10)$$

$$a_{x2}=v_{x2}-v_{x1}/t_2-t_1 \quad (11)$$

$$a_{xj}=(v_{xj}-v_{xj-1})/(t_j-t_{j-1}),\ \text{for}\ j\in N\geq 1 \quad (12)$$

From (15), the value for v_{xj} is extracted:

$$v_{xj}=a_{xj}(t_j-t_{j-1})+v_{xj-1} \quad (13)$$

$$v_{xj}=\Delta v_{xj}+v_{xj-1} \quad (14)$$

The raw inertial acceleration signal contains measurement errors in the range of $\pm 0.02(m/s^2)$.

Drift is observed in figure 9 and is caused by integration of read errors $err_{n.x}$ (10). Although only speed measurements are required for our purpose, by further integrating the speed signal, the position can be obtained. The drift would further be amplified and the simulated signal value would drift quickly from the real value.

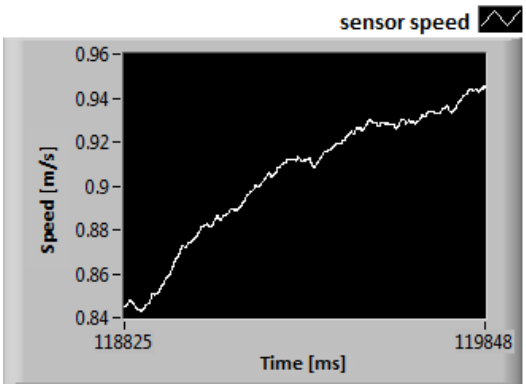

Fig. 9. Sensor speed data obtained by integrating the sensor acceleration data.

EXPERIMENTAL RESULTS

Linear speed is obtained both from the sensor on the mobile device and encoders on the electric vehicle wheel motors: the first one, by integrating the sensor linear acceleration and the second one by derivating wheel motor position. In figure 10, the vehicle accelerates until a constant speed of −0.3(rad/s) is achieved. Note that this is not reverse movement; the negative value is due to inverse position of the right motor with respect to the left motor; same shaft axis, opposite rotational direction.

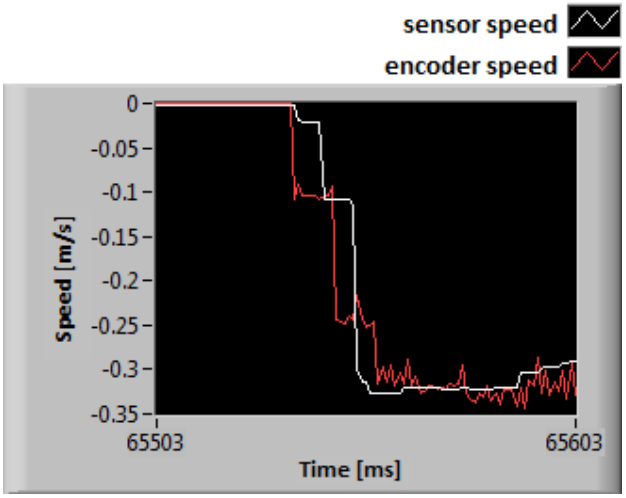

Fig. 10. Measured sensor and encoder speed (m/s), obtained by integrating sensor acceleration and derivating encoder position, respectively. Acceleration phase is shown.

The first period of positive wheel slip for the vehicle lasts for 15(ms), until the 65545(ms) mark: λ = 0.8 The second one is shorter, only lasts 5(ms) until the 65550(ms) mark with smaller slip: λ = 0.56. Negative slip (wheel block) is observed from 65550 to 65560(ms), λ = −0.32. After this point in time, slip stabilizes to a value close to zero.

CONCLUSIONS

✓ Gravitational component is determined using Euler angles. It then must be removed from raw acceleration sensor data to obtain inertial acceleration.

✓ Inertial acceleration data is transformed into vehicle speed data and compared to wheel speed to measure wheel slip.

✓ Slip is visible at acceleration from standstill, in three jerking movements of the wheel.

✓ To better visualize the wheel slip and the effect of the slip control, changes are proposed. In the future, the slip coefficient value will be forced to rise by

changing to a road surface with low adhesion coefficient and by changing the wheel tire surface with a more slippery one, like plastic instead of rubber.

BIBLIOGRAPHY

1. **Jazar, R., N.,** "Vehicle Dynamics. Theory and Aplication", Springer, 2008.
2. **Hori, Y., Toyoda, Y., Tsuruoka Y.,** "Traction Control of Electrical Vehicle based on the Estimation of Road Surface Condition – Basic Experimental Results using the Test EV 'UOT Electric March'", Power Conversion Conference - Nagaoka, 1997.
3. **Bräunl T.,** "Embedded Robotics", Springer, 2003.
4. *Guide to the Measurement of Mass and Weight.* http://www.bis.gov.uk/assets/nmo/docs/faqs/calibration/calculation-of-g.pdf
5. *Calibration Of iPhone Accelerometers.* http://rouel-projects.blogspot.ro/p/calibration-of-iphone-accelerometers.html

About the authors

Eng. **Daniel SZÖCS,** PhD candidate
Technical University of Cluj-Napoca
email:daniel.szocs@edr.utcluj.ro

Electrical Engineer of the Technical University of Cluj-Napoca, Department of Electrical Machines and Drives. Currently is a third year PhD candidate. From 2011 has done research for the doctoral thesis at National Instruments Romania, the hardware basis for the research has been National Instrument Robotics Starter Kit. Research topics: direct-drive electrical vehicles, anti-slip control.

Eng. **Andrei FENEȘAN,** PhD candidate
Technical University of Cluj-Napoca
email:daniel.szocs@edr.utcluj.ro

Electrical Engineer of the Technical University of Cluj-Napoca, Department of Electrical Machines and Drives. A second year PhD candidate. Research topics: direct-drive electrical vehicles, obstacle avoidance, trajectory control with LADAR and GPS technology.

Prof. Eng. **Teodor PANĂ,** PhD
Technical University of Cluj-Napoca
email:teodor.pana@edr.utcluj.ro

Professor of Microprocessor and Computer Systems and two other digital control based courses at the Technical University of Cluj-Napoca, Faculty of Electrical Engineering. Head of the Department of Electrical Machines and Drives. He has four books published in Romania, fourteen published articles in engineering publications and over 70 papers published at international conferences. Research topics: vector control systems, electric vehicle drive control, industrial robots.